FLORIDA STATE UNIVERSITY

COLLEGE OF ARTS AND SCIENCES

THE VARIABILITY OF THE WET SEASON OVER SOUTHEAST ASIA

By

ALICE S. BRENNAN

A Thesis submitted to the
Department of Earth, Ocean, and Atmospheric Science
in partial fulfillment of the
requirements for the degree of
Master of Meteorology

2024

Alice Brennan defended this thesis on May 24, 2024.
The members of the supervisory committee were:

Vasubandhu Misra
Professor Directing Thesis

Mark Bourassa
Committee Member

Michael Diamond
Committee Member

The Graduate School has verified and approved the above-named committee members and certifies that the thesis has been approved in accordance with university requirements.

I want to dedicate this thesis to my mother (Angela Brennan); my late father (Denis Brennan); and my partner (Robert Mancuso). I also want to dedicate this work to all the friends I have made and colleagues I have worked with during my time at Florida State University. I thank you for believing in me, and as a result, helping me to believe in myself.

ACKNOWLEDGMENTS

We acknowledge the support from NASA grant 80NSSC22K0595. IMERG dataset was provided by the NASA/Goddard Space Flight Center, alongside the PPS which developed and computed the IMERGE as a contribution to GPM and archived at the NASA GES DISC.

I also want to acknowledge the support of Dr. Vasubandhu Misra, C.B. Jayasankar, and Joanna Rodgers for all their help with this project.

TABLE OF CONTENTS

LIST OF FIGURES

ABSTRACT

The Southeast Asian (SEA) region experiences a rainy season during boreal spring and summer, which the SEA population relies on for agricultural and economic development. This study uses an objective definition for the onset and demise date for the seasonal evolution of the rainy season over the SEA region. The onset and demise dates are defined as the first and last date of the year when the daily rain rate reaches a maximum and minimum cumulative anomaly of the mean climatological rainfall rate, respectively. This gives rise to a varying length of the season that has a significant impact on the estimate of the seasonal rainfall and its anomaly over the rainy season. It is observed that the interannual variability of the seasonal rainfall of the rainy season is significantly affected by the variations of the onset and demise dates. However, the influence of the onset and demise date appears to be independent of each other. Using the Integrated Multi-Satellite Retrievals for Global Precipitation Mission version 6 (IMERG) rainfall analysis available on 0.1°x0.1°grid we have analyzed the variations of the rainy season over SEA. We generate an ensemble of 101 members per season in the 22-year time period by slightly perturbing the original time series to account for uncertainties in the observed rainfall analyses. This also ensures that the diagnoses of the onset/demise dates are not sensitive to sporadic synoptic/mesoscale rain events that may be unconnected to the seasonal evolution of rainfall in SEA. Using this ensemble of 101 members per season, we find that we can provide a reliable probabilistic outlook of the forthcoming rainy season over the SEA region based on the variations of the onset date of the wet season. This is possible because of the strong intrinsic relationship of earlier or later onset seasons of the SEA rainy season associated with a longer and wetter season, or a shorter and drier season, respectively.

CHAPTER 1

INTRODUCTION

1.1 Southeast Asian Region

The Southeast Asia (SEA) region harbors a population of over 691 million people, and as such, is a dominant contributor to global agriculture and economic productivity (WorldoMeters 2024). The domain is situated between two oceans (the Indian and Pacific) and is influenced by a multitude of oceanic and atmospheric teleconnections, such as the Indian Ocean Dipole (IOD), intraseasonal oscillations (ISO), the Madden Julian Oscillation (MJO), and the El Niño Southern Oscillation (ENSO) (Saji et al. 1999; Xie et al. 1963; Madden and Julian 1971; Kembell-Cook and Wang 2001; Walker and Bliss 1932; NOAA 2024). The seasonal variations of the winds, accompanied by differences in the land-ocean temperature contrast, lead to a monsoonal climate in the region (NOAA 2024). Typically, in the relatively dry boreal winter, the SEA terrain cools faster than the water in the Indian Ocean, due to its lower specific heat. As a result of this, the near surface winds blow away from the land, out to the ocean, due to the pressure gradient. Conversely, during the boreal summer, the land warms faster than the ocean, and the winds begin to blow from the Indian Ocean onto the SEA region as the pressure gradient reverses direction (Costa et al. 2023).

There is an array of monsoonal patterns that affect regions within and surrounding the tropics. Depending on the literature, the Asian monsoon can be separated into three categories: the Indian/South Asian summer monsoon, the East Asian summer monsoon, and the SEA Monsoon (Wang and LinHo 2002; Misra and DiNapoli 2013). This study exclusively targets the SEA monsoon, which includes the following countries: Myanmar, Thailand, Laos, Cambodia, Vietnam, and peninsular Malaysia. We calculated and determined four parameters for every monsoonal season from 2001-2022 in the region that will be analyzed throughout the study: onset date of the monsoon season, demise date of the monsoon season, length of the monsoon season, and seasonal rain totals (Rodgers 2023).

Figure 1.1 The geographical domain of Southeast Asia (SEA) used in this study. From Google Earth (2024).

1.2 SEA Monsoon Onset and Demise

A typical SEA monsoonal season begins around late May and ends in September (Lau and Yang 1997; Costa et al. 2023). The majority of the region has a seasonal length ranging from 120-160 days, which is most of the boreal summer season (Misra and DiNapoli 2013). Given the large latitudinal extent of the region, there is considerable variation in the evolution of the SEA monsoon. For example, southern SEA (peninsular Malaysia), which is located closer to the equator in comparison to northern SEA (including Myanmar, Laos, Vietnam, Cambodia, and Thailand) has two wet seasons. There is a wet season during the boreal summer, the same season as the rest of SEA, and a dominating wet season in boreal winter, with Indonesia and the Maritime Continent (Chang et al. 2005).

A key component in the monsoonal pattern is the Inter-Tropical Convergence Zone (ITCZ), which is an area of tropical convergence caused by the upward motion of the Hadley cell in this region. During the boreal winter, the ITCZ shifts south of the equator, and during boreal summer, the ITCZ shifts north of the equator (Hadley 1735; Fig. 1.2). In boreal winter, as illustrated in the left panel in Figure 1.2, the peninsula Malaysia region is more influenced by the boreal winter monsoon when the surface winds turn northeasterly (Krishnamurti 1971; IPCC 2014). The boreal winter monsoon, similar to the boreal summer monsoon, is characterized as the wet season

occurring between November-February due to a wind reversal, as northeasterly flow blows over the South China Sea due to high pressure over land (Chen et al. 2013). When the ITCZ shifts northward during the summertime, as illustrated in the right-hand picture of Figure 1.2, the northern portions of SEA (Thailand, Myanmar, Laos, Cambodia, and Vietnam) are more directly influenced by southwesterly winds (Geen et al. 2020).

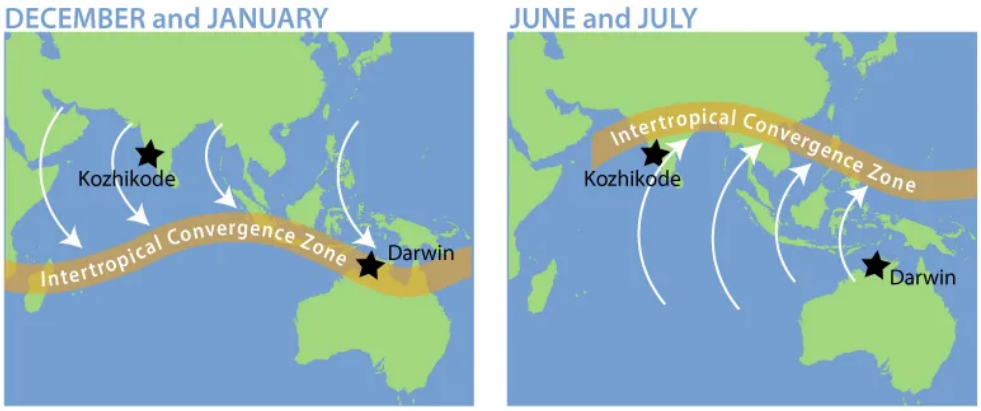

Figure 1.2 ITCZ shift in boreal winter (left panel) and boreal summer (right panel). From the University Corporation of Atmospheric Research (2024)

Some other notable atmospheric features in the region, as seen in Figure 1.3, include the Mascarene High, located around 20°S and 60°E. This is a semi-permanent pressure system in the southern Indian Ocean, providing anti-cyclonic circulation (Behera and Yamagata 2001). This counterclockwise flow can merge with the tropical Southeast trade winds. Key local features north of the equator in the upper atmosphere are the Somali Jet (also known as the Findlander Jet), which is a low-level cross-equatorial flow pattern that shifts westerly on the eastern edge of the African continent, and the tropical easterly jet (TEJ), an upper-level easterly wind stream that blows from the Tibetan High (Krishnamurti et al. 2013; Misra 2023).

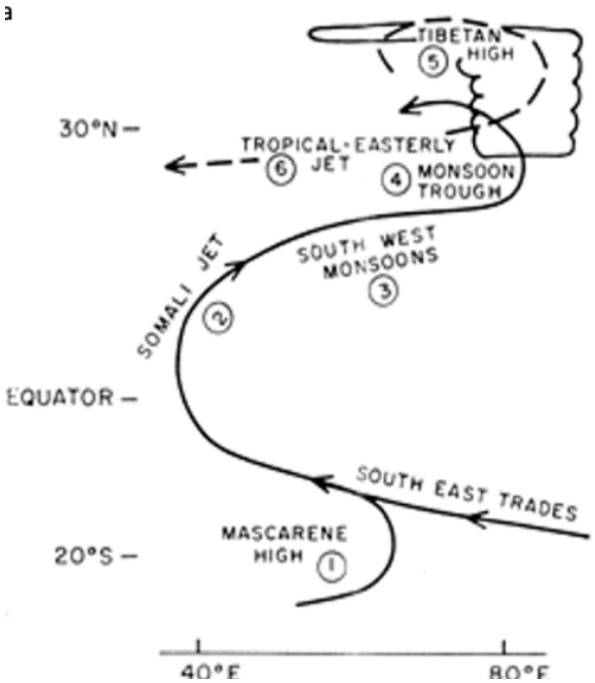

Figure 1.3 Schematic of the characteristic flows of the Indian Summer monsoon and the climatological means in boreal summer. From Krishnamurti et al. (2013)

The Indonesian Throughflow (ITF) is a water pathway that connects the western Pacific Ocean to the Indian Ocean and is a critical component of transporting western Pacific waters into the tropical eastern Indian Ocean (Wyrtki 1987; Godfrey 1996; Schneider 1998; Lee et al. 2002; Vranes et al. 2002; Sprintall et al. 2014). The ITF is primarily caused by a sea level pressure difference that occurs between the two oceans and can result in a westward shift in the Pacific warm pool, causing the eastern Indian Ocean Sea surface temperatures (SSTs) to rise (Wyrtki 1987; Schneider 1998; Misra 2023). The western Pacific waters that the ITF depends on are heavily influenced by the Walker Circulation, which is a zonal circulation that influences wind patterns and ocean flow across the Pacific Ocean (Bjerknes 1969). During El Niño years, when there is weakened Walker Circulation, the ITF goes through the Makassar Strait (a water channel between Kalimantan and Sulawesi within the Indonesian archipelago) and weakens, resulting in a shallow thermocline (Sprintall et al. 2014; Misra 2023). The SEA monsoon can impact the waters going through the Karimata Strait towards the Java Sea, which can cause a “freshwater plug” for the ITF and impact its seasonality (Lee at al. 2019).

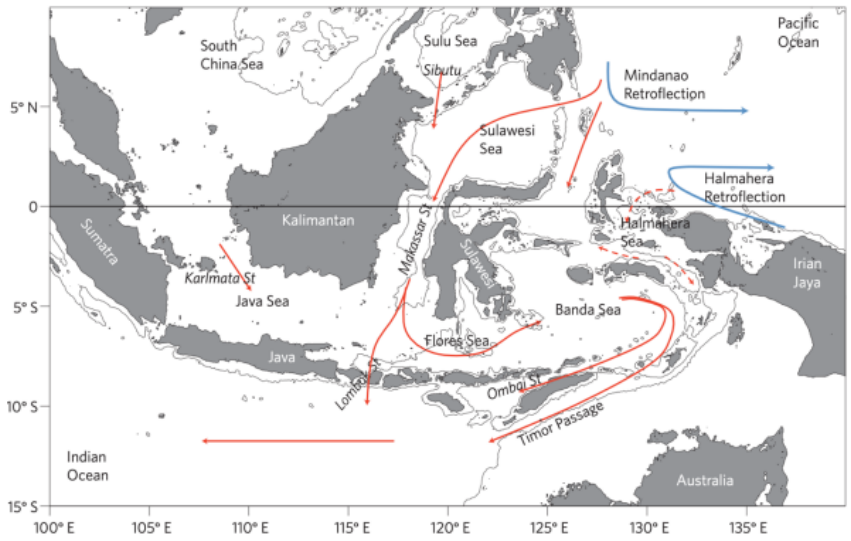

Figure 1.4 Indonesian throughflow (solid red lines) and the South Pacific contribution to the throughflow (dashed red lines). From Sprintall et al. (2014)

1.3 Teleconnections

In terms of large-scale atmospheric processes, SEA is influenced by ENSO (Ropelewski and Halpert 1987; Kripalani and Kulkarni 1998; Hguyen-Thanh et al. 2023; Xu et al. 2023) and the IOD (Pillai et al. 2020). The ENSO pattern is an interannual teleconnection pattern that affects the strength of the Walker Circulation. When the Walker circulation weakens during the warm ENSO phase, the associated equatorial easterly winds weaken, and cause there to be anomalous subsidence over the SEA surface. As a result, these weakened trade winds will have less influence in transporting surface waters westward over the eastern Pacific, causing an accumulation of warm water in the eastern Pacific Ocean due to less upwelling. Conversely, when the Walker circulation is strengthened during the cold ENSO phase, there is anomalous convergence over the SEA surface (NOAA 2024). As a result of this enhanced convergence, the monsoon is strengthened during La Niña events, and weakened during El Niño events (Lin et al. 2024).

The Indian Ocean Dipole (IOD) is an aperiodic oscillation that affects sea surface temperatures SSTs within the Indian Ocean (Saji et al. 1999). A neutral IOD phase occurs when there are no statistically significant temperature anomalies in the Indian Ocean, and equatorial trade winds at the surface blow westerly. In a positive IOD phase, anomalously easterly equatorial winds blow over Indian Ocean surface, causing a warm SST anomaly and enhanced convection in

the western portion of the Indian Ocean, and a cold SST anomaly in the eastern portion of the ocean. Conversely, during the negative IOD phase, strong equatorial anomalous westerly winds, making the western portion of the ocean have a cold SST anomaly and the eastern portion have a warm SST anomaly, leading to enhanced precipitation and convection in SEA (Misra 2023; NOAA 2024). IOD events typically develop in boreal summer and strengthen in boreal autumn, and depending on the strength of the dipole, can intensify monsoonal trends or weaken them (Jiang et al. 2021).

1.4 Previous Studies

A similar study conducted by Misra and DiNapoli (2013) looked at the seasonality of the rainy season in the Southeast and South Asian monsoons from 1951-2007. The data for their project came from the APHRODITE project that gridded fine-scale resolution data at a 40km grid resolution from discrete rain gauge observations (Yatagai et. al 2012). Misra and DiNapoli (2013) concluded that the SEA region has the longest wet season in comparison to all of the other Asian monsoonal regions, as the variations in the onset/demise can, independently of one another, influence the length of the monsoon season. They also concluded that earlier than average monsoon onset dates were associated with a stronger than average summer seasonal Somali jet.

This study also follows Rodgers (2023), which utilized the same data set and methodology to research the defined onset, demise, length, and rain totals over the Central America region. Their paper studied the correlation of these parameters with the ENSO cycle, alongside the Atlantic warm pool and East Pacific Warm Pool. They found that the monsoonal pattern over the region is weakly correlated with the large-scale teleconnections in both ocean basins, but the variability in the onset date impacts the length and rain total values in the region, indicating a benefit to utilizing the onset date variations to predict future season patterns. We wanted to expand on this project by applying this methodology to SEA and seeing if there is a similar pattern in climatological teleconnections influencing the season start/finish dates, which in turn could influence its predictability.

1.5 Objectives

Following previous studies (Liebmann and Marengo 2001; Misra and DiNapoli 2014; Dunning et al. 2016; Uehling and Misra 2020; Rodgers and Misra 2023), the goal of this report is to pinpoint the seasonal variations of the monsoon season onset dates, demise dates, length of the season, and rain totals over SEA. We intend to utilize this determination of the onset date to predict the length of the monsoon season and expected rain totals. The benefit of this study is to evaluate the predictability of anomalous monsoon seasons based on the onset date of the rainy season, which in turn, can prove beneficial for the populations' preparations.

CHAPTER 2

METHODS

2.1 Precipitation & SST Data

This project uses daily rainfall from the National Aeronautics and Space Administration (NASA)'s Integrated Multi-satellite Retrievals for Global Precipitation Mission (IMERG) version 6. IMERG collected daily rainfall data from multi-satellite platforms that were launched into space in March 2014 as a part of the Global Precipitation Mission (GPM). The IMERG data set uses a half-hourly temporal resolution alongside a 0.1°x0.1° grid resolution and provides data from June 2000 to the present. This study's temporal range is 1 January 2001 to 31 December 2022. The IMERG rainfall data is obtained from 3 different rainfall analysis runs: early, late, and final. The early runs have a 4-hour latency; late runs have a 14-hour latency; and final runs have a 3.5-month latency (Rodgers 2023). These various latencies are utilized due to the way satellite radiance data processes and provide quality control. The late run of this data set was used in this project to benefit from the preprocessing (as compared to the early run), alongside having real-time applications without compromising data accuracy (Huffman et al. 2019).

This project also utilizes SST data from the NOAA Optimal Interpolation SST (OISST2; Huang et al. 2021) analysis version 2.1, which is a daily analysis of SST data ranging from 1982 to present on a 0.5°x0.5° resolution scale. From this SST data, IOD and ENSO indices were created, using seasonally averaged values over 10°S-10°N and 120°W-170°W, within the Niño3.4 region, following the methodology of Huang et al. 2015 and the NOAA CPC Oceanic Nino Index. The three indexes for the ENSO/IOD SSTs included in this study were chosen based on boreal season definitions: December, January, and February (DJF); March, April, and May (MAM); June, July, and August (JJA). The DJF season used December from the previous year to create the DJF, means used in this study for assessing the correlations to the rainy season. These observations were taken from SST observations via satellites, ships, and buoys. The rest of the ocean basins not covered by observations are then filled in with statistical interpolation methods (optimum interpolation), so there is a temperature reading per grid point (Reynolds et al. 2007).

2.2 Methodology

The onset date of the rainy season is defined as the first day of the year when the cumulative daily rain rate exceeds the annual mean climatological rain rate. The cumulative curve anomaly is computed by subtracting the annual mean climatological rain rate from the daily rain rate (Rodgers 2023). To determine this date objectively, we plot the daily cumulative anomaly curve and identify the first inflection point (Fig. 2.1). Similarly, the demise date of the rainy season is identified as the second inflection point in the cumulative anomaly curve (Fig. 2.1). For example, Fig. 2.1 illustrates the onset and demise of the wet season for rain rates averaged over Vietnam in 2001. Once the onset date is reached on Julian Day 116, the cumulative anomaly curve increases and continues to become more positive until the demise day is reached beyond which the curve begins to decline on Julian Day 300 (Fig. 2.1).

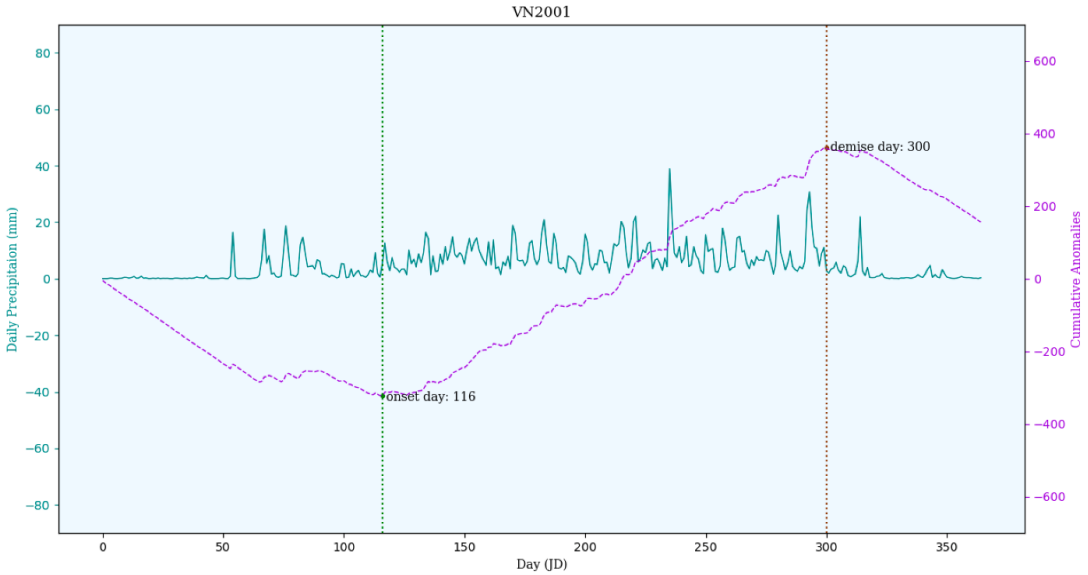

Figure 2.1 The daily rainfall totals (mm) and cumulative anomalies (mm) in Vietnam during 2001. The left y-axis is daily precipitation in mm, representing the blue line on the plot, while the right-hand side y-axis is the cumulative anomalies, which represents the dashed purple line on the plot. The vertically dotted green line going through the data is the onset date, and the vertically dotted brown line going through the data is the demise date.

Mathematically, the cumulative anomaly curve is represented as:

$$C'_m(i) = \sum_{n=1}^{i} [A_m(n) - \bar{\bar{C}}] \quad (1)$$

$$\bar{\bar{C}} = \frac{1}{MN} \sum_{m=1}^{M} \sum_{n=1}^{N} A(m,n) \quad (2)$$

Where $C'_m(i)$ is the cumulative anomaly of the rainfall average mean for the year (m) on the day (i). $A_m(n)$is the amount of rainfall in the year (m) on the day (n). In equation 2, $\bar{\bar{C}}$ is the climatology of the average rainfall mean over *N* (number of days in the year, which is either 365 or 366 for a Leap Year), and *M* is the number of years. Utilizing these two formulas, plots for every year ranging from 2001-2022 for each of the six countries within the study region were generated in order to find the onset and demise dates.

In order to ensure that the cumulative anomaly onset and demise dates are reasonable, a range of accepted dates is created. From the 22 onset/demise dates for each year, the median of the onset, demise, length, and rain totals for each year are taken and a 30 day onset/demise "window", or threshold, is centered on the median value and is determined to set a "normal" value that can be utilized for comparing each country's rainy season. For example, the median onset date for Myanmar was Julian Day 133, so the onset date window was Julian Days 118-148. To obtain a range for the entire SEA region, we used the earliest onset date window value, which was in Thailand, and latest demise date window, which was in Myanmar. This then resulted in a range between Julian Days 79 and 148. Similarly, the earliest demise date window, which was in Laos, and the latest demise date window, located in Vietnam, resulted in a final window range between Julian Day 259 and 315. The corresponding seasonal length values are calculated by subtracting the demise date from the onset date. Seasonal rain totals are calculated by adding the rain total amounts starting at the onset date and ending on the demise date of the rainy season.

To account for any uncertainty within the rainfall data, a perturbation method, similar to a bootstrapping method, was applied (Misra et al. 2023). This method takes the original daily rainfall values time series and replaces the values with a random rainfall value within -3 to +3 days for every date, in order to account for any mesoscale/synoptic scale disturbances. A variety of studies have been conducted and suggest that there is a significant amount of mesoscale to synoptic scale precipitation events in SEA (Stensrud 1996; Zipser et al. 2006; Liu and Zipser 2016). This process is then repeated 100 times to provide a 101-iteration time-series (100 perturbed time series alongside the original time series) to create an ensemble of estimates for the onset and demise dates of the monsoon season, following the method of Rodgers et al. (2023).

Pearson correlation tests are used to evaluate the strength/weakness of the linear relationships amongst the onset, demise, length, and rain totals and the teleconnection patterns. Then, significance at the 95% level confidence interval is calculated utilizing a two-tailed t-test. It

is critical to note, however, that a t-test does not account for the false discovery rate that is often realized when a large set of correlations are tested simultaneously (Livezey and Chen 1983; Benjamini and Hochberg 1995).

The variation of the monsoonal onset date has been shown to have a strong linear relationship with the season's length and rainfall anomalies (DiNapoli and Misra 2013). In order to test the probabilistic skill of the onset date to forecast the seasonal outlook, we use the area operating characteristic curve (AROC) following Misra (2004), Narosky and Misra (2021), and Rodgers (2023). To calculate these AROC scores, the onset dates are categorized as being early, normal, or late, based on tercile thresholds. Similarly, the length is categorized as being either long, normal, or short. Seasonal rain totals are categorized as either wet, normal, or dry. For this study, we are specifically looking for the following 4 events: early onset associated with a wetter season; early onset associated with a longer season; late-onset associated with a drier season; late onset associated with a shorter season. Utilizing the 101 ensemble members per year data, the onset dates are then separated based on whether they are considered early, normal, or late.

Table 1 Contingency table used for generating the relative operating characteristic (ROC) curves to quantify forecast uncertainty. Reproduced from Narotsky and Misra 2021.

	When the ensemble probability for the event EXCEEDS threshold	**When the ensemble probability for the event DOES NOT EXCEED threshold**
Event occurs	Hit (H)	Miss (M)
Event does not occur	False Alarm (FA)	Correct Rejection (CR)

Within each year, all of the ensemble members are sorted into a contingency table (Table 1). If the event (i.e., the monsoon) does not occur, but all of the ensemble members of the seasonal outlook are categorized as occurring for said event exceeds the threshold (which is from 0%-100%), the event is considered a False Alarm (FA). If the event does not occur in observations, and the ensemble members of the seasonal outlook does not exceed the threshold, the event is Correctly Rejected (CR). If the event occurs in observations and the ensemble members of the seasonal outlook that categorized that event as occurring exceeds the threshold, that event is considered a Hit (H). If the event occurs but the ensemble members do not exceed the threshold, it is considered a Miss (M) (Rodgers and Misra 2023). For each ensemble member, the H, M, FA,

and CR are added together over the 22-year time period, and the following equations are used to calculate the HR and FAR:

$$HR = \frac{H}{H + M}$$

$$FAR = \frac{FA}{FA + CR}$$

These two parameters, HR and FAR, are then plotted against one another as a scatter plot to produce the AROC curve. An AROC score ranging from 0-.49 indicates low to no predictability (i.e., a random forecast has better prediction skill), and an AROC score of .5-1 indicates there is good predictability to the event (i.e., indicating the parameter forecasts better than a random forecast).

CHAPTER 3

RESULTS AND DISCUSSION

The first portion of the results focuses on the climatological values from 2001-2022 in six countries within SEA: Myanmar, Thailand, Cambodia, Laos, Vietnam, and Malaysia.

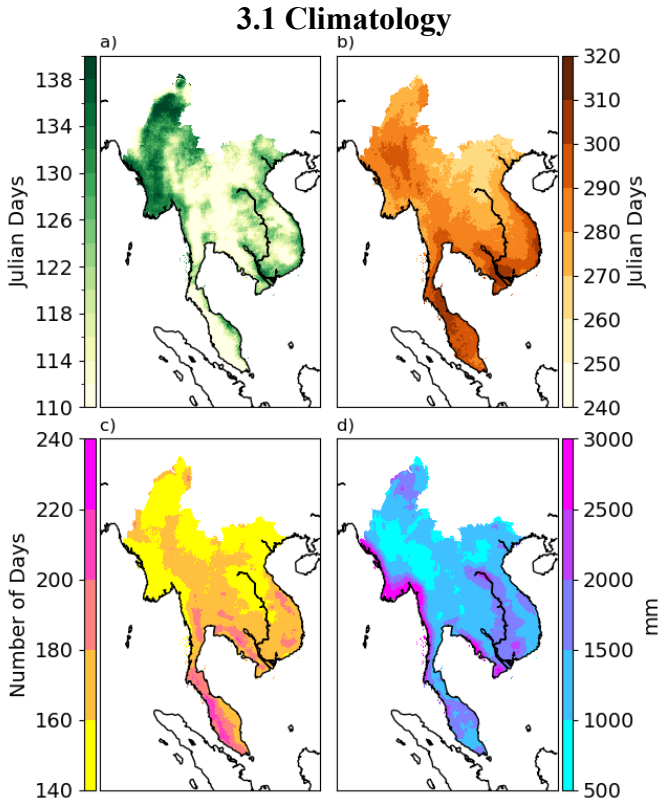

Figure 3.1 The climatological median: a) onset date (Julian Days), b) demise date (Julian Days), c) seasonal length (days), and d) seasonal rain from IMERG.

Figure 3.1a shows the spatial variation of the onset dates in SEA. Coastal regions alongside countries closer to the equator (i.e. Malaysia and southern Thailand), tend to have earlier onsets around Julian Day 90 (which is around March 31st). Considering that the ITCZ shifts northward during boreal spring (Fig. 1.2), equatorial regions are going to be influenced by the convectively enhanced region of the ITCZ due to increased moisture inflow and low-level convergence earlier in the season. There are also earlier onset dates in the middle of the SEA region, such as in inner Thailand and Laos. These specific areas are south of the Xiangkhoang Plateau and the Chaing Mai Plateau in Thailand, both of which span over 6,000m in altitude (Fig. 1.1; Google Earth 2024). Areas north of the plateaus have later onsets, as the leeward side of the elevated surface is going

to hinder vertical convective development that can result in convection and precipitation, as the orographic lifting can make the air parcel precipitate all the internal moisture out on the windward side of the feature, resulting in dry air developing and descending down the leeward side of the geographical feature. Additionally, it can be noted that the majority of Myanmar experiences a later onset, which may be due to its northern location.

As for demise dates in SEA, it is observed in Figure 3.1b that areas with an earlier onset tend to have a later demise of the rainy season. This is distinguishable in Malaysia and Thailand, which are both coastal, alongside being south of the various plateaus in the area. Similarly, the locations with an early demise are where there was typically have a late onset date, such as Myanmar and elevated portions of Laos. These demise dates range from Julian Day 260 (September 17th) to 310 (November 23rd). Consequently, the shortest monsoonal season seems to be in Myanmar and central Laos, regions west and east of the areas with the longest monsoonal seasons. In terms of rain totals, despite having the shortest monsoon season, the coast of Myanmar gets upwards of 3,500 mm of rain during the rainy season – that's roughly 137 inches! In this case, the large rainfall totals, despite Myanmar having a relatively shorter monsoon season, can be attributed to higher daily rainfall rates than some of the other regions in SEA with longer seasons. Northern and inland areas of Myanmar get the least amount of rain, which is around 500mm (or 19 inches).

Figure 3.2 displays the corresponding standard deviation values for these parameters for the rainy season in SEA. Examining the onset dates in Fig. 3.2a, the lowest standard deviation range for onset dates is in Myanmar, especially near the coastal and northern portions of the country (Fig. 3.2a). Outside of Myanmar, the majority of SEA has a broader range of onset date variability, with the largest variability of about +/-30 days in northern Myanmar, northern Vietnam, and portions of peninsular Malaysia. For demise dates, inland Laos and mountainous portions of Myanmar have the least amount of variability compared to the higher variations in southernmost Malaysia (Fig 3.2b). The seasonal length has quite a varying spatial distribution, with the smallest standard deviations in length being over most of Myanmar, coastal Vietnam, and Laos, with a 10-day variation. The largest standard deviation in seasonal length is in northern Myanmar, inland Vietnam, and southern Malaysia. Northern Myanmar is affected by the westerly jet (or the subtropical jet that gets split by the Tibetan Plateau) which can cause an increase in convective storms roaming in the area (Seman 2023). This is further supported by the standard

deviations of the rain totals, with northern Myanmar having high variability, alongside coastal Myanmar and coastal Thailand. Similarly, enhanced precipitation amounts around the coast and northern areas of Myanmar can be attributed to the Arakan Yoma Mountain to the north and south, respectively, resulting in orographic precipitation (Shige et al. 2017). Peninsular Malaysia sees some more rain variability since it is coastal, more equatorial, and impacted by a variety of tropical wave disturbances (Kembell-Cook and Wang 2001).

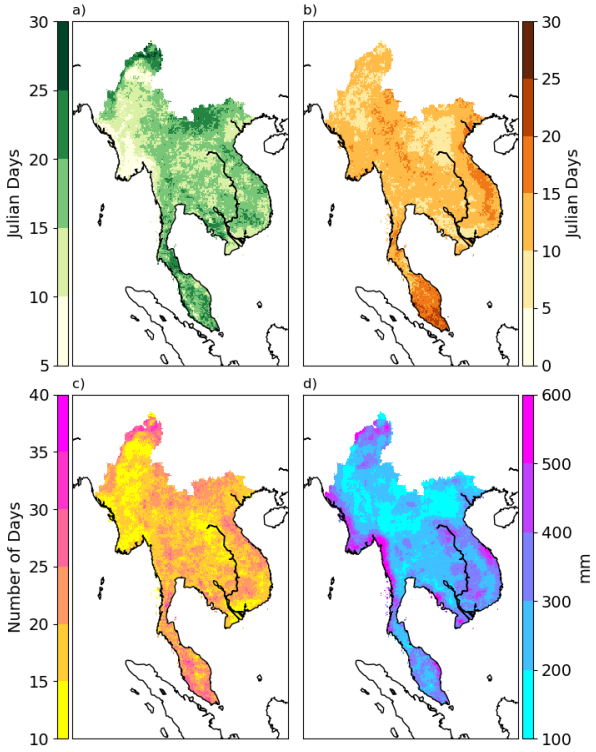

Figure 3.2 The standard deviation of (a) onset date (days), (b) demise date (days), (c) length (days), and (d) seasonal rain (mm) of the wet season.

Figure 3.3 illustrates the climatological area-averaged daily rainfall for all six countries within SEA from 2001-2022. Peninsular Malaysia stands out immediately, portrayed by the bright red line above, as being much more uniform compared to the rest of the countries in SEA. This particular country gets a large amount of rainfall due to its proximity to the equator and tropical wave disturbances local to the Indian Ocean (i.e., the ITCZ shifting north and south of this region in boreal summer and winter, respectively, and the MJO).To explain why there is only one peak in peninsular Malaysia, since this country experiences two rainy seasons, it is important to note

that this study is specifically looking at the boreal summer SEA monsoon, generally ranging from April – October. Typically, however, peninsular Malaysia has another wet season in boreal winter, which explains the flat nature of the seasonal rain totals. The onset and demise of the rainy season are difficult to identify because peninsular Malaysia is not in its primary wet monsoon season until later in the year. The most extreme "-peak" in daily average rainfall, after peninsular Malaysia, occurs in Cambodia and Myanmar, which makes sense as in Figure 3.1d it can be noted how extreme the precipitation was in the coastal regions of these countries. Laos, Thailand, and Vietnam display similar climatological daily rain rate profiles to one another.

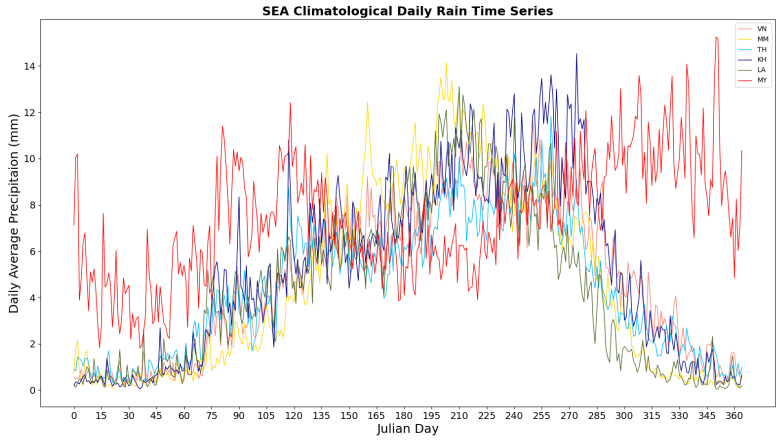

Figure 3.3 The climatological daily time series of rainfall (mm/day) for a) Vietnam (VN), b) Myanmar (MM), c) Thailand (TH), d) Cambodia (KH), e) Laos (LA), and f) Malaysia (MY) from IMERG observations during 2001-2022.

Figure 3.4 correlates the onset with length and rain, demise with length and rain totals, and lastly, the onset with the demise. The goal here is to see if the onset or demise is better correlated with length and/or rain totals to provide increasingly reliable seasonal forecasts. It is important to note, however, from a statistical perspective, that Figure 3a and 3c involve cross-correlations, as the length of the monsoon season is being correlated to the onset and demise, both of which are required to determine how long the season is. This can cause an overestimation, depending on how significantly the onset of the monsoon depends on the demise.

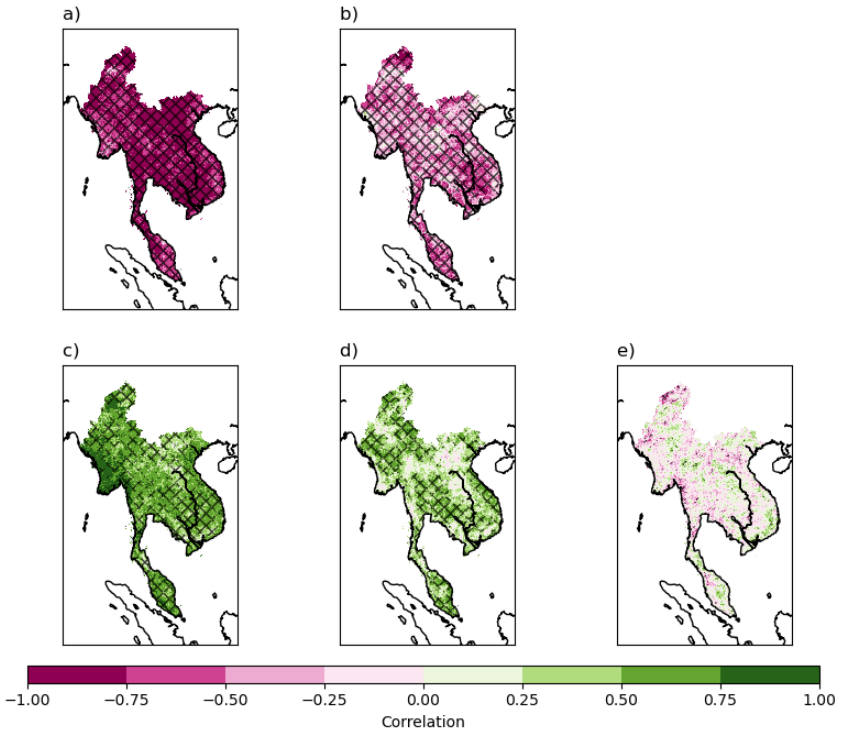

Figure 3.4 Correlation of a) onset with length b) onset with rain totals c) demise with length d) demise with rain totals, and e) onset with the demise. Statistically significant data at the 95th percentile is hatched in black.

For the onset and length, everywhere in the region is significantly and negatively correlated, so the earlier (later) the onset date, the longer (shorter) the length. Daily rainfall rates during the season are not necessarily related to the variation in onset dates. That being said, seasonal rainfall anomalies can be influenced by variations in the season length and daily rain rates. There are outside factors that can influence the rain totals, such as ENSO, IOD, terrain, ' Similar to Figure 3.8a, 3.8c indicates that there is a strong positive relationship between demise dates and season length. These positive correlations suggest that the earlier (later) the demise day the shorter (longer) the season. Coastal Myanmar has the strongest feedback for this relationship. There is, however, a weaker correlation between the rain totals and demise date as compared to the onset date and the rain. Lastly, the onset and demise date correlation relationship are very low and sporadic in location, with no statistical significance. Since the onset and demise have weak and spatially noisy dependence on one another, the cross-correlation noted in Figures 3.4a and 3.4c are only slightly overestimated. The conclusion drawn from this is that we cannot confidently use the onset date of the rainy season to predict the end date of the monsoon. The onset date is a

better predictor for how anomalous the monsoonal seasonal length or rain totals will be compared to the climatological average.

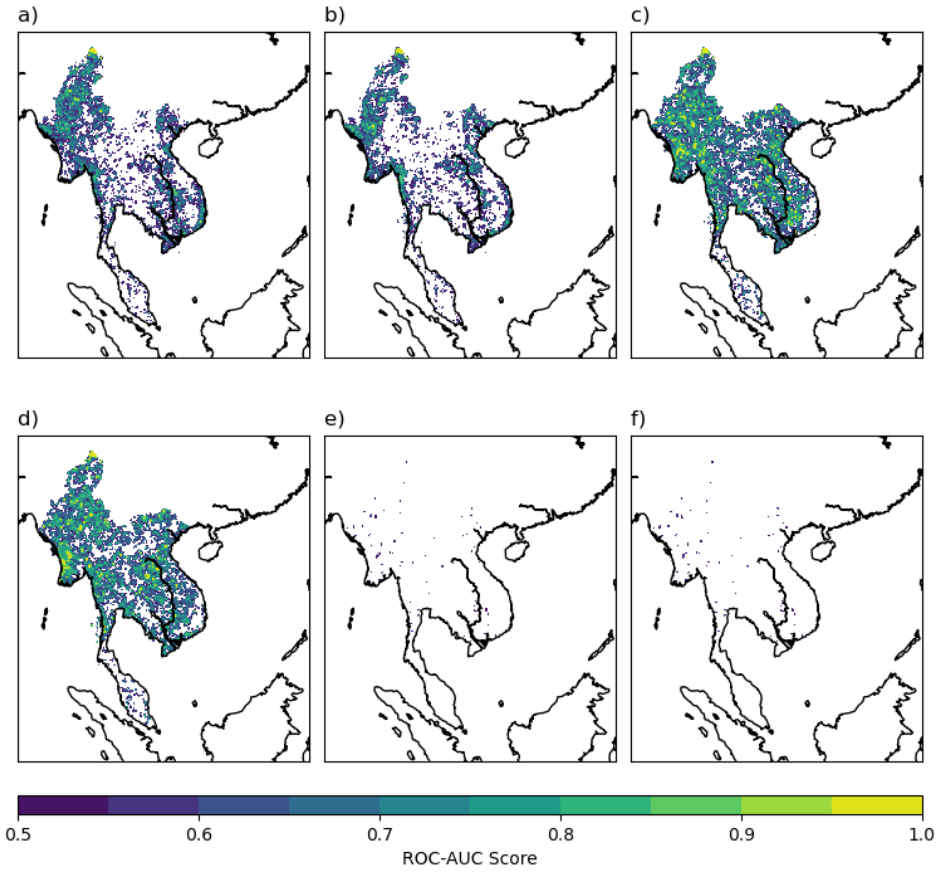

Figure 3.5 The area under the relative operating characteristic curve (AUROC) for the outlook of a) a longer, wet season b) a wetter wet season, c) a shorter wet season, d) a drier wet season, e) a normal length wet season, and f) a normal wet season rainfall based on the normal start of the wet season. Regions shaded signify AUROC >= 0.5, indicating regions with probabilistic skill that is better than a random forecast.

Figure 3.5 correlates the onset with length and rain, demise with length and rain totals, and lastly, the onset with the demise. The goal here is to see if the onset or demise is better correlated with length and/or rain totals to provide increasingly reliable seasonal forecasts. For the onset and length, everywhere in the region is significantly and negatively correlated, so the earlier (later) the onset date, the longer (shorter) the length. Daily rainfall rates during the season are not necessarily related to the variation in onset dates. That being said, seasonal rainfall anomalies can be influenced by variations in the season length and daily rain rates. There are outside factors that can influence the rain totals, such as ENSO, IOD, terrain, etc. Similar to Figure 3.5a, 3.5c indicates that there is a strong positive relationship between demise dates and season length. These positive

correlations suggest that the earlier (later) the demise day the shorter (longer) the season. Coastal Myanmar has the strongest feedback for this relationship. There is, however, a weaker correlation between the rain totals and demise date as compared to the onset date and the rain. Lastly, the onset and demise date correlation relationship are very low and sporadic in location, with no statistical significance. The conclusion drawn from this is that we cannot confidently use the onset date of the rainy season to predict the end date of the monsoon. The onset date is a better predictor for how anomalous the monsoon season is expected to be, which can provide insight on if there is going to be more or less rain on average compared to the climatological average.

From a forecasting standpoint, it is important to look at how these plots differ from one another. Comparing Figure 3.4 and 3.5, Figure 3.5 provides a more fine-grained outlook for each country so that citizens in each portion of the region can note how the start of the monsoon impacts each country individually. From figures 3.5a and 3.5c, it can be noted that the earlier the onset, the lower the ROC scores, in comparison to later onset scores. The highest early onset scores occur in inland Myanmar and portions of Vietnam, indicating these areas can expect a longer and or wetter season if there is an early monsoon start date. ROC scores are higher in Cambodia, Laos, Thailand and coastal Myanmar have higher confidence in a late onset start causing a dry and or short season.

3.2 ENSO & IOD Correlations

We also examined the local teleconnections within the SEA domain during the rainy season. Figure 3.6 is for the December, January, and February (DJF) Niño 3.4 index correlations with each of the monsoon season parameters. Boreal winter is when the ENSO variability is at its peak in the equatorial Atlantic. Looking at the plots in Figure 3.6, it can be noted that ENSO patterns are not as strong as the correlations seen in Figure 3.4. There is a statistically significant positive correlation between the onset of the rainy season over the elevated region inland of Thailand, coastal Vietnam, and the northern Malaysia Peninsula with the DJF ENSO index. This indicates that when the ENSO pattern is warm (cold), the onset date is expected to be later (earlier). During La Nina, the Walker Circulation is enhanced, causing an increase in SST values in the western Pacific, which can fuel the convective development and moisture content for the SEA region during monsoon season. Conversely, during El Nino, the Walker circulation is suppressed, causing a decrease in SST values in the western Pacific, which would not be favorable for the SEA rainy

season. This corresponds to figure 3.5, as it was illustrated that an earlier onset date (corresponding to La Nina) can lead to a wetter and or longer season. These same locations have statistically significant negative correlations for the demise and DJF ENSO index. This indicates that when the ENSO pattern is warm (cold), the demise date is expected to be earlier (later). Figure 3.6c shows negative correlations between the length of the season and DJF ENSO index. Seasonal length values are significant over the Amaka Yoma mountains in Myanmar, but very weak. Likewise, correlations with seasonal rain totals and the DJF ENSO index are spatially incoherent and weak (Fig. 3.6d).

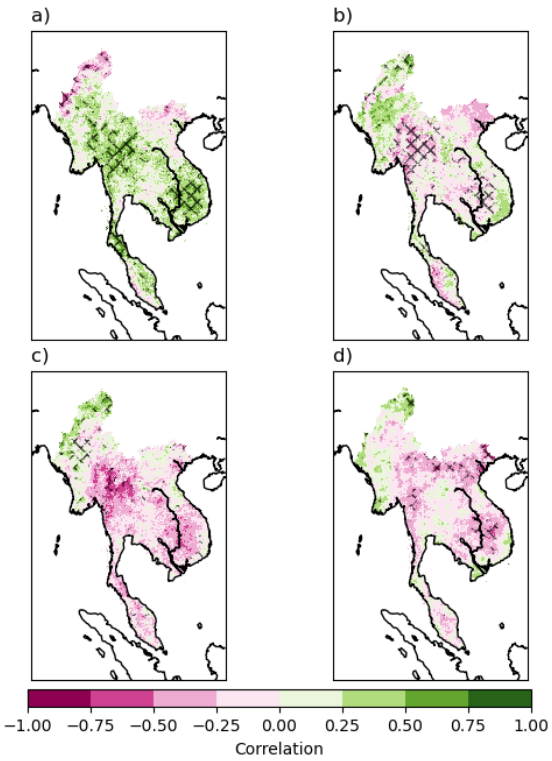

Figure 3.6 The correlation of preceding DJF Niño3.4 SST index (OISSTv2; Reynolds et al. 2002) with anomalies of (a) onset date, (b) demise date, (c) seasonal length, and (d) seasonal rain of the rainy season. Statistically significant data at the 95th percentile is hatched in black.

Similarly, we examine the SSTs for the March, April, and May (MAM) ENSO index with the onset date, demise date, season length, and season rain totals over the SEA region (Fig. 3.7). The MAM ENSO index has a positive correlation with onset dates over the majority of SEA, indicating that during the warm or cold ENSO phase, onset dates appear to be earlier or later, respectively. There is a relatively small negative correlation between coastal peninsula Malaysia

and inland Myanmar (Fig 3.7a). Correlations between the MAM ENSO index and the monsoon demise dates are more sporadic, with only inland Myanmar and eastern coastal Vietnam displaying statistical significance (Fig 3.7b). Northeastern Vietnam and parts of Cambodia have a negative correlation, signaling that during warm (cold) ENSO phases, the demise date occurs earlier (later). Correlations are very weak, spatially sporadic, not statistically significant between the MAM ENSO index and seasonal length (Figure 3.7c). The correlations between the MAM ENSO index and the seasonal rain totals, however, are negative and statistically significant within Cambodia and inland Vietnam (Figure 3.7d). This is further supported by Figure 3.5, again, as La Nina events seem to cause earlier onset dates, which is typically associated with a projected longer and wet rainy season.

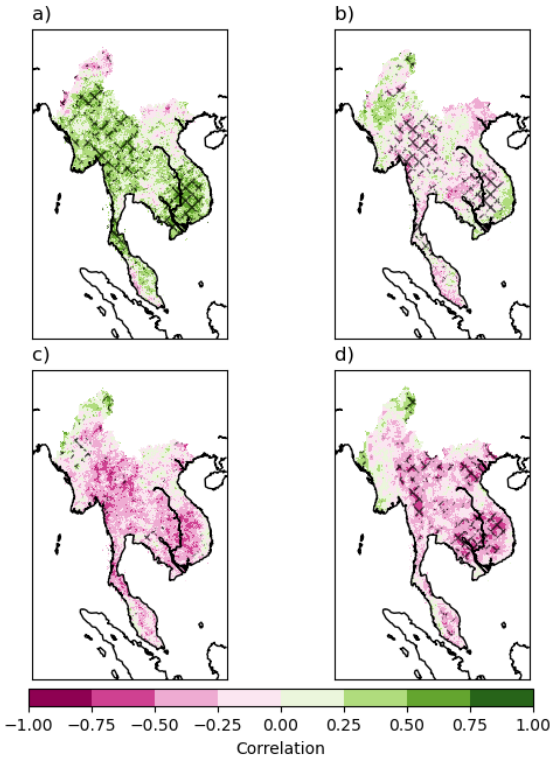

Figure 3.7 The correlation of concurrent MAM Niño3.4 SST index (OISSTv2; Reynolds et al. 2002) with anomalies of (a) onset date, (b) demise date, (c) seasonal length, and (d) seasonal rain of the rainy season. Statistically significant data at the 95th percentile is hatched in black.

The JJA ENSO index and the onset dates show no statistical significance and have spatially sporadic correlation values (Fig. 3.8a). JJA ENSO index and demise dates display similar results, in terms of a lack of statistical significance, except there is one negative statistically significant region in Vietnam (Fig 3.8b). Generally, areas with a positive (negative) correlation for onset dates and JJA ENSO index, appear to have a negative (positive) correlation with the demise

date and the JJA ENSO index. Similarly, the length of the rainy season correlated to the JJA ENSO index is weak and spatially random, with a negative statistically significant relationship over inland Vietnam (Fig 3.8c). Lastly, rain totals and the JJA ENSO index correlations are mostly negative, with statistical significance in Cambodia and Vietnam (Fig 3.8d). Myanmar's coast, however, signals a positive correlation with the JJA ENSO index, but has no statistical significance (Fig 3.8d).

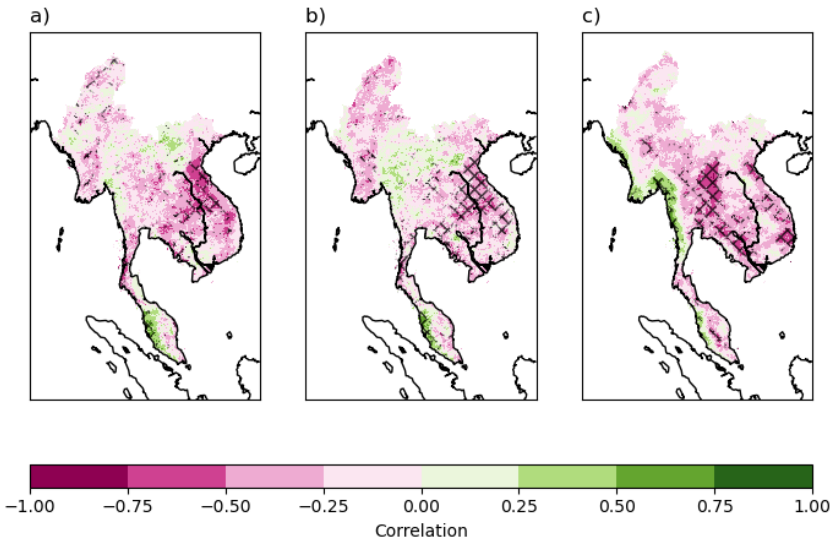

Figure 3.8 The correlation of concurrent JJA Niño3.4 SST index (OISSTv2; Reynolds et al. 2002) with anomalies of (a) demise date, (b) seasonal length, and (c) seasonal rain of the rainy season. Statistically significant data at the 95th percentile is hatched in black.

In Figure 3.9, we look at the teleconnection of the SEA rainy season with the SON seasonally averaged IOD index. IOD index and onset date relationships are not plotted in Figure 3.13, because the IOD follows almost two seasons after the onset of the rainy season. The demise date has weak but statistically significant negative correlations throughout the majority of Vietnam, Cambodia, Laos, and inland Myanmar with the IOD index, indicating that during positive, or negative, phases of the IOD, the demise dates occur earlier, or later, respectively (Figure 3.9a). During the negative phase of the IOD, the Indian Ocean has anomalously warm waters in the east, which is co-located with SEA. The warm SSTs are a benefit to monsoon moisture and convective development. A similar relationship is observed for the IOD index and length of the season, as any significant values are all negatively correlated with one another and are weak, indicating negative IOD phases correspond to longer seasons. (Fig 3.9b). IOD index and seasonal rain values are stronger in comparison to the onset and season length panels in Figures

3.9and 3.9b, with statistical significance in Cambodia and Vietnam, showing higher rain totals falling during negative phase IOD events (Figure 3.9c). There are positive correlations on coastal Thailand, but they lack significance (Fig 3.9c).

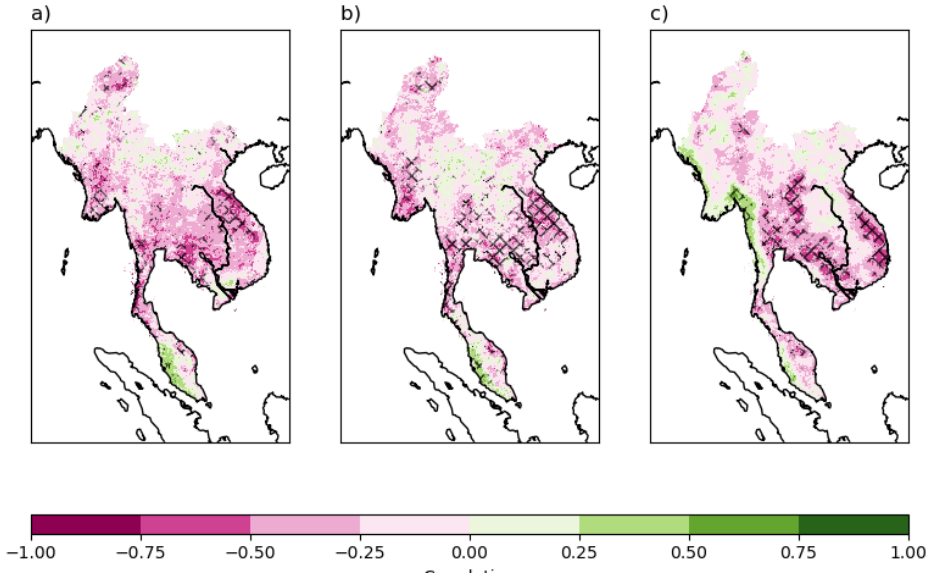

Figure 3.9 The correlation of the preceding IOD index (OISSTv2; Reynolds et al. 2002) with the median (a) demise date, (b) seasonal length, and (c) seasonal rain of the rainy season. Statistically significant data at the 95th percentile is hatched in black.

CHAPTER 4

CONCLUSIONS

Southeast Asia is a vastly geographically diverse region with a plethora of plateaus, rivers, and mountains, which naturally impact the rainy season. With a high population density and continuous socio-economic development, there is a growing need for reliable monsoon predictions. The methods used in this study utilized a differing perspective of the onset, demise, seasonal length, and rain totals from IMERG daily time series rainfall observations, which show the rainy season trends on a regionally averaged scale, alongside an individual grid point scale. Despite there being evidence of ENSO and IOD influencing the SEA monsoon, predicting just how influential proves to be challenging due to complex land-sea interaction causing large inherent variability.

Our research highlights how monitoring the onset of the wet season in SEA can provide valuable insights for monsoonal forecasts. Relationships between the onset dates with the length and rain values are very strong and show remarkably high levels of correlation. The SEA onset date plays a larger role in impacting the length and rain totals of the monsoonal season, as opposed to climate phenomena such as ENSO and the IOD. An early (late) onset date is associated with a longer or wetter (shorter or drier) monsoon season, further indicating a strong relationship between the onset dates and seasonal outcomes (Fig. 3.4). As a result, continued monitoring of these monsoonal patterns would be beneficial to locals and government officials in the SEA region to continue to increase the predictability of the monsoon, which in turn will increase the nation's ability to prepare for the rainy season. By applying this study's definition for the onset and demise of the season, alongside observing the correlations between the onset date and length/rain totals, this report can prove to be highly valuable for forecasting the monsoon season for the SEA population.

This study utilized code and methodology that has been successfully utilized in past case studies of precipitation trends over Florida, India, Australia, and Central America. (Liebman and Marengo 2001; DiNapoli and Misra 2014; Dunning et al. 2016; Uehling and Misra 2020; Narotsky and Misra 2021; Rodgers and Misra 2023). This study can be further utilized to investigate the precipitation patterns anywhere in the world and is currently being used in a study for Africa. Some future projects that could be interesting to build from this would be investigating the Madden-

Julian Oscillation correlation with this region's length and rain totals since it has a strong influence on convection in the area. Similarly, there would be a benefit in utilizing this methodology for the winter monsoon, which is Malaysia and the Maritime Continent's predominant wet season.

REFERENCES

Banzon, V., R. Reynolds, and National Center for Atmospheric Research Staff (Eds), 2022: The Climate Data Guide: SST data: NOAA Optimal Interpolation (OI) SST Analysis, Version 2 (OISSTv2) 1x1. Accessed 4 June 2024, https://climatedataguide.ucar.edu/climate-data/sst-data-noaa-optimal-interpolation-oi-sst-analysis-version-2-oisstv2-1x1.

Behera, S.K., T. Yamagata, 2001: Subtropical SST dipole events in the southern Indian Ocean. Am. Geophysical Union. *International J. Climate*, **42** (9), 4700=4715. https://doi.org/10.1002/joc.7498

Benjamini, Y., and Y., Hochberg, 1995: Controlling the false discovery rate: A practical and powerful approach to multiple testing. *Journal of the Royal Statistical Society: Series B*, **57**(1), 289-300. https://doi.org/10.1111/j.2517-6161.1995.tb02031.x

Bjerknes, J., 1969: Atmospheric teleconnections from the equatorial Pacific. *Mon. Wea. Rev*., **97**, 163–172.

Bureau of Meteorology, 2024; Indian Ocean. Accessed 11 April 2024, http://www.bom.gov.au/climate/about/australian-climate-influences.shtml?bookmark=iod

Chabangborn, A., 2014: Asian Monsoon over Mainland Southeast Asia in the 25,000 Years. Accessed 4 June 2024, https://www.semanticscholar.org/paper/Asian-monsoon-over-mainland-Southeast-Asia-in-the-Chabangborn/b16ceda61524bb6c9ef97809d4921fd8217490ee

Chang, C. -P., Z. Wang, H. Hendon, 2006: The Asian Winter Monsoon. *Springer Link*, The Asian Monsoon 89-127. https://doi.org/10.1007/3-540-37722-0_3

Chang, C., Z. Wang, J. McBride, and C. Liu, 2005: Annual Cycle of Southeast Asia—Maritime Continent Rainfall and the Asymmetric Monsoon Transition. *J. Climate*, **18**, 287–301, https://doi.org/10.1175/JCLI-3257.1.

Chen, T., J. Tsay, M. Yen, and J. Matsumoto, 2013: The Winter Rainfall of Malaysia. *J. Climate*, **26**, 936–958, https://doi.org/10.1175/JCLI-D-12-00174.1.

Cherchi, A., and Coauthors, 2021: Annex V: Monsoons in Climate Change 2021: The Physical Science Basis. Contribution of Working Group I to the Sixth Assessment Report of the Intergovernmental Panel on Climate Change, *IPCC*, pp. 2193–2204, doi:10.1017/9781009157896.019.

Costa, H., and Coauthors, 2023: Monsoon. Accessed 11 April 2024, https://education.nationalgeographic.org/resource/monsoon/

Dunning, C.M., E.C.L. Black, and R.P. Allan, 2016: The onset and cessation of seasonal rainfall over Africa. *J. Geophy. Res. Atmos*., **121**, 11, 405-11,424, https://doi.org/10.1002/2016JD025428

Fountain, H., Khandelwal, S., Levitt, Z., White, J., O'Neill, 2022; The Monsoon Is Becoming More Extreme. Accessed 11 April 2024, https://www.nytimes.com/interactive/2022/10/04/climate/south-asia-monsoon-climate-change.html

Geen, R., S., Bordoni, D.S., Battisti, and K., Hui, 2020: Monsoons, ITCZs, and the concept of the global monsoon. *Reviews of Geophysics*, **58**, https://doi.org/10.1029/2020RG000700

Godfrey, J. S, 1996: The effect of the Indonesian Throughflow on ocean circulation and heat exchange with the atmosphere: A review, *J. Geophys. Res*., **101**, 12,217–12,237.

Hadley, G., 1735: Concerning the cause of the general trade-winds. *Philo. Trans*., 29, 58-62.

Huang, B., M., L'Heureux, Z.Z., Hu., H.M., Zhang, 2015. Ranking the strongest ENSO events while incorporating SST uncertainty. *Geophy. Res. Letters*, **43,** 9165-9172, doi:10.1002/2016GL070888.

Huang, B., and Coauthors, 2015: Extended Reconstructed Sea Surface Temperature Version 4 (ERSST.v4). Part I: Upgrades and Intercomparisons. *J. Climate*, **28**, 911–930, https://doi.org/10.1175/JCLI-D-14-00006.1.

Huang, B., C. Liu, V. Banzon, E. Freeman, G. Graham, B. Hankins, T. Smith, and H. Zhang, 2021: Improvements of the Daily Optimum Interpolation Sea Surface Temperature (DOISST) Version 2.1. *J. Climate*, 34, 2923–2939, https://doi.org/10.1175/JCLI-D-20-0166.1.

Huffman, G.J., E.F., Stocker, D.T., Bolvin, E.J., Nelkin, and J., Tan, 2019: Integrated multi-satelittE retrievals for GPM (IMERG) technical documentation. *NASA/GSFC Code*, 612(47), 2019.

Jiang, J., Y. Liu, J. Mao, J. Li, S. Zhao, and Y. Yu, 2022: Three Types of Positive Indian Ocean Dipoles and Their Relationships with the South Asian Summer Monsoon. *J. Climate*, **35**, 405–424, https://doi.org/10.1175/JCLI-D-21-0089.1.

Kemball-Cook, S. and B. Wang, 2001: Equatorial waves and air-sea interaction in the Boreal summer intraseasonal oscillation. *J. Climate*, **14**, 2923-2942.

Lau, K., and M. Li, 1984: The Monsoon of East Asia and its Global Associations—A Survey. Bull. *Amer. Meteor. Soc.,* **65**, 114–125, https://doi.org/10.1175/1520-0477(1984)065<0114: TMOEAA>2.0.CO;2.

Lau, K.M., and S. Yang, 1997: Climatology and Interannual Variability of the Southeast Asian Summer Monsoon. Advances in Atmos. Sci., 14(2). https://doi.org/10.1007/s00376-997-0016-y Liebmann, B., and J. Marengo, 2001: Interannual Variability of the Rainy Season and Rainfall in the Brazilian Amazon Basin. *J. Climate*, **14**, 4308–4318, https://doi.org/10.1175/1520-0442(2001)014<4308: IVOTRS>2.0.CO;2.

Lee, T., I. Fukumori, D. Menemenlis, Z. Xing, and L. Fu, 2002: Effects of the Indonesian Throughflow on the Pacific and Indian Oceans. *J. Phys. Oceanogr*., **32**, 1404–1429, https://doi.org/10.1175/1520-0485(2002)032<1404:EOTITO>2.0.CO;2.

Lee, T., S., Fournier, A.L., Gordon, and Coauthors, 2019: Maritime Continent water cycle regulates low-latitude chokepoint of global ocean circulation. *Nat Commun 10*, 2103. https://doi.org/10.1038/s41467-019-10109-z

Lin, S., B., Dong, S., Yang, 2024: Enhanced impacts of ENSO on the Southeast Asian summer Monsoon Under Global Warming and Associated Mechanisms. *Am. Geological Society*. **51**, 2. https://doi.org/10.1029/2023GL106437

Liu, C., and E.J. Zipser, 2015: The global distribution of largest, deepest, and most intense precipitation systems. *Geophys. Res. Lett*., https://doi.org/10.1002/2015GL063776

Livezey, R. E., and W. Y. Chen, 1983: Statistical Field Significance and its Determination by Monte Carlo Techniques. *Mon. Wea. Rev*., **111**, 46–59, https://doi.org/10.1175/1520-0493(1983)111<0046:SFSAID>2.0.CO;2.

NASA, 1993: Eclipse Bulletins (Southeast Asia). Accessed 4 June 2024, https://eclipse.gsfc.nasa.gov/SEpubs/19951024/text/weather-southeast-asia.html

Madden, R.A., and P.R. Julian, 1971: Detection of a 40-50 day oscillation in the zonal wind in the tropical Pacific *J. Atmos. Sci*., **28**, 702-708.

Masiwal, R., V. Dixit, and A. K. Seshadri, 2023: Explaining Dynamics and Rapid Onset of the Somali Jet through Its Kinetic Energy Budget. *J. Atmos. Sci*., **80**, 833–847, https://doi.org/10.1175/JAS-D-22-0160.1.

Misra, V., 2023: An Introduction to Large-Scale Tropical Meteorology. *Springer Atmospheric Sciences*. 282 pp.

Misra, V., and S. DiNapoli, 2014: The variability of the Southeast Asian summer monsoon. *Int. J. Climatol.,***34**(3), 893-901, https://doi.org/10.1002/joc.3735.

Narotsky, C. D. and V. Misra 2022: The Seasonal Predictability of the Wet Season over Peninsular Florida *Int. J. Climatol*., https://doi.org/10.1002/joc.7423.https://doi.org/10.1002/joc.7423.

Nguyen-Thanh, H., T., Ngo-Duc, and M., Herrmann, 2023: The distinct impacts of the two types of ENSO on rainfall variability over Southeast Asia. *Clim Dyn* 61, 2155–2172. https://doi.org/10.1007/s00382-023-06673-2

NASA, 2023. IMERG V07 Technical Documentation. Accessed 4 June 2024, https://gpm.nasa.gov/resources/documents/imerg-v07-technical-documentation

NOAA, El Nino & La Nina (El Nino – Southern Oscillation). Accessed 5 May 2024, https://www.climate.gov/enso

NOAA, 2023; Inter-Tropical Convergence Zone. Accessed 11 April 2024, https://www.noaa.gov/jetstream/tropical/convergence-zone

NOAA, 2024: What Is a Monsoon? Accessed 11 April 2024, https://scijinks.gov/what-is-a-monsoon/

Pillai, P.A., D.A., Ramu, and R.C., Nair, 2021: Recent changes in the major modes of Asian summer monsoon rainfall: influence of ENSO-IOD relationship. *Theor Appl Climatol* 143, 869–881. https://doi.org/10.1007/s00704-020-03454-3

P.J., V., and Coauthors. 2020: Global warming hiatus contributed weakening of the Mascarene High in the Southern Indian Ocean. Sci Rep 10, 325. https://doi.org/10.1038/s41598-020-59964-7

Rodgers, J., 2023: The Characterization of the Variability of the Wet Season Over Central South America.

Roldán-Gómez, P. J., J.F., González-Rouco, C., Melo-Aguilar, and J.E., Smerdon, 2022: The role of internal variability in ITCZ changes over the Last Millennium. *Geophysical Research Letters,* **49**, 4. https://doi.org/10.1029/2021GL096487

Ropelewski, C. F., and M. S. Halpert, 1987: Global and Regional Scale Precipitation Patterns Associated with the El Niño/Southern Oscillation. *Mon. Wea. Rev.,* **115**, 1606–1626, https://doi.org/10.1175/1520-0493(1987)115<1606:GARSPP>2.0.CO;2.

Safari, M.A.M., N., Masseran, M.H.A., Majid, 2022: Wind energy potential assessment using Weibull distribution with various numerical estimation methods: a case study in Mersing and Port Dickson, Malaysia. *Theor Appl Climatol* **148**, 1085–1110. https://doi.org/10.1007/s00704-022-03990

Saji, N. H., B.N. Goswami, P.N. Vinayachandran, and T. Yamagata, 1999: A dipole mode in the tropical Indian Ocean, *Nature,* **401**, 360-363.

Sang, Y.F., V.P., Singh, and K., Xu, 2019: Evolution of IOD-ENSO relationship at multiple time scales. *Theor Appl Climatol* **136**, 1303–1309. https://doi.org/10.1007/s00704-018-2557-7

Schneider, N., 1998: The Indonesian Throughflow and the Global Climate System. *J. Climate*, **11**, 676–689, https://doi.org/10.1175/1520-0442(1998)011<0676:TITATG>2.0.CO;2.

Seman, S., D., Babb, L.M., Grenchi, 2023: The Subtropical Jet Stream. Accessed 05 May 2024. https://www.e-education.psu.edu/meteo3/l11_p6.html

Stensrud, D. J., 1996: Importance of Low-Level Jets to Climate: A Review. *J. Climate*, **9**, 1698–1711, https://doi.org/10.1175/1520-0442(1996)009<1698:IOLLJT>2.0.CO;2.

Uehling, J. and V. Misra, 2020: Characterizing the seasonal cycle of the Northern Australian rainy season. *J. Climate*, **33**, 8957-8973.

Ventura, V., C. J. Paciorek, and J. S. Risbey, 2004: Controlling the Proportion of Falsely Rejected Hypotheses when Conducting Multiple Tests with Climatological Data. *J. Climate*, **17**, 4343–4356, https://doi.org/10.1175/3199.1.

Verma, S., R., Bhatla, and P.K., Singh, 2024: Understanding the Association of Tropical SST Anomalies on the ISMR During Extreme IOD Events. *Pure Appl. Geophys*. **181**, 373–389. https://doi.org/10.1007/s00024-023-03394-9

Vranes, K., A.L., Gordon, and A. Ffielf, 2002. The heat transport of the Indonesian Throughflow and implications for the Indian Ocean heat budget. Deep Sea Research Part 11: *Tropical Studies in Oceanography,* **49,** 1391-1410. https://doi.org/10.1016/S0967-0645(01)00150-3

Walker, G.T., and E.W. Bliss, 1932: *World Weather V. Memoirs of the Royal Meteorological Society*, **4**, 53-84.

Wang, B., and LinHo, 2002: Rainy Season of the Asian–Pacific Summer Monsoon. *J. Climat*e, **15**, 386–398, https://doi.org/10.1175/1520-0442(2002)015<0386:RSOTAP>2.0.CO;2.

Worldometer, 2024. Population of South-Eastern Asia. Accessed 05 May 2024, Population of South-Eastern Asia (2024) - Worldometer (worldometers.info)

Wyrtki, K., 1987: Indonesian through flow and the associated pressure gradient. *J. Geophys. Res.,* **92**, 12 94112 946, https://doi.org/10.1029/JC092iC12p12941.

Xie, Y.-B., S.-J. Chen, I.-L. Zhang, and Y.-L. Hung, 1963: A preliminary statistic and synoptic study about the basic currents over southeastern Asia and the initiation of typhoon (in Chinese). *Acta Meteor. Sin*., **33**, 206-217.

Xu, C., S.Y.S.,Wang, K., Borhara, 2023: Asian-Australian summer monsoons linkage to ENSO strengthened by global warming. *Clim Atmos Sci* **6**, 8. https://doi.org/10.1038/s41612-023-00341-2

Zipser, E. J., D. J. Cecil, C. Liu, S. W. Nesbitt, and D. P. Yorty, 2006: WHERE ARE THE MOST INTENSE THUNDERSTORMS ON EARTH?. *Bull. Amer. Meteor. Soc*., **87**, 1057–1072, https://doi.org/10.1175/BAMS-87-8-1057.

BIOGRAPHICAL SKETCH

Alice Sarah Brennan was born in Mineola, New York in 2000 to her parents Angela and Denis Brennan. She attended the State University of New York (SUNY) Oneonta for her undergraduate career, where she had a volunteer position with the National Weather Service and was the instrumentation intern for the rooftop observation equipment during her senior year. In May 2022, she graduated from SUNY Oneonta, earning a Bachelor of Science in meteorology and a Bachelor of Arts in English. In August 2022, she began her graduate studies at Florida State University, where she is pursuing a Master of Science in meteorology. During her time at Florida State University, Alice worked as a teaching assistant and eventually lead teaching assistant for introductory meteorology labs, alongside working with Dr. Vasubandhu Misra studying the variations in the Southeast Asian monsoon.